Micromachined passive waveguide fabrication with fs laser in Ag-doped GeO_2–PbO glasses for photonics: straight, curved and Y shaped configurations

Thiago Vecchi Fernandes
Departamento de Engenharia de Sistemas Eletrônicos
Escola Politécnica da USP
São Paulo, Brazil
thiago.vecchi.f@hotmail.com

Camila D. S. Bordon
Departamento de Engenharia de Sistemas Eletrônicos
Escola Politécnica da USP
São Paulo, Brazil
camiladvieira@gmail.com

Niklaus U. Wetter
Centro de Lasers e Aplicações, Instituto de Pesquisas Energéticas e Nucleares
IPEN-CNEN
São Paulo, Brazil
nuwetter.ipen@gmail.com

Wagner de Rossi
Centro de Lasers e Aplicações, Instituto de Pesquisas Energéticas e Nucleares
IPEN-CNEN
São Paulo, Brazil
wderossi@gmail.com

Luciana R. P. Kassab
Departamento de Ensino Geral
Faculdade de Tecnologia de São Paulo
São Paulo, Brazil
kassablm@osite.com.br

2024 38th Symposium on Microelectronics Technology and Devices (SBMicro) | 979-8-3315-4063-0/24/$31.00 ©2024 IEEE | DOI: 10.1109/SBMicro64348.2024.10673876

ABSTRACT — This study aims to produce and characterize different dual waveguides using femtosecond (fs) laser irradiation on GeO_2-based glass samples. The work is motivated by previous results obtained with rare earth ions doped GeO_2 – PbO glass, with and without silver nanoparticles, in which irradiation, with fs laser was successful. The work aims to manufacture different structures such as straight, curved, and Y waveguides (using the double guide configuration) for applications in photonics (resonant rings, beam splitters, among others) in GeO_2 – PbO glasses with silver nanoparticles. For both, straight and S curved waveguides, better M^2 (beam quality factor) results were found for a distance between the guide walls of 10 µm, when compared to 25 µm. Moreover, among the two different curved guides produced it was also possible to observe better guidance when a larger radius of curvature (20 mm) was used; preliminary tests showed no guiding for 5 mm and 10 mm radius. The highest relative propagation loss was obtained for the S curved waveguide with a 25 µm distance between the guide walls whereas the lowest one was found for the Y shaped waveguide; for this configuration (opening angle of 5° and distance of 620 µm between the two arms) an output power ratio between the left and right arm of 53.9/46.1 showed promising applications for beam splitters.

Keywords **—** germanate glasses, femtosecond laser, double guides, curved guides, Y guides.

I. INTRODUCTION

GeO_2-PbO glasses feature a low phonon energy (800 ~ 975 cm^{-1}), wide transmission window (400 ~ 4500 nm), high refractive index (2.0) associated with the high atomic mass of the elements and high polarizability, good chemical, thermal and mechanical stabilities, low melting point compared to silicate glasses, low glass transition temperature and good solubility of rare earth ions (TRs) [1, 2]. GeO_2-PbO glasses doped with TRs demonstrated enhanced optical properties due to the plasmonic effects of metallic NPs [3]. Moreover, these glasses with metallic NPs exhibited significant potential for photonic applications due to their ultrafast response times and high third-order nonlinearities [4]. The first results of dual-line waveguides written by femtosecond (fs) laser and produced directly in glasses based on GeO_2 and TeO_2 were reported in [5]. More recently, we showed a new configuration of dual-line waveguides, produced in Nd^{3+} doped GeO_2-PbO glass containing silver (Ag) nanoparticles (NPs), for applications in optical amplifiers at 1064 nm [6,7]. Inspired by these promising results, which showed improved beam quality factor and optical gain, we present for the first time the production of dual-line waveguides with diverse configurations such as, straight, curved [8, 9], and Y-shaped [10, 11], by using GeO_2-PbO glasses with Ag NPs. These guides were directly inscribed via femtosecond laser onto the glasses, for applications in photonic devices, such as resonant rings [12], high gain amplifiers [8], beam splitters [13], among others. We utilized a Ti:Sapphire femtosecond (fs) laser operating at 800 nm, which delivered 30 fs pulses at a 10 kHz repetition rate. We present results of beam quality factor M^2 (at 632 and 1064 nm), propagation loss and polarization. The present result covers a lack in the literature as there are few reports of waveguides inscribed in glasses with Ag NPs by fs laser [10]. Another contribution of the present investigation is the use of glasses for curved and Y waveguide configurations as mainly of the reports are produced in crystalline hosts.

II. MATERIALS AND METHODS

The glass manufacturing process involved the original composition (in wt%) $40GeO_2$-60PbO (labeled GP) with the addition of 2.0 wt% $AgNO_3$. The samples were prepared using the melt quenching technique. The process involved the melting of the reagents in high purity alumina crucible (99.999%) at 1200 °C, using a glass rod for homogenization. Subsequently, the molten material was poured into preheated brass molds, followed by annealing at 420 °C for 1 hour. This procedure is crucial to reduce

internal tensions and provide greater resistance to the samples. After annealing, the samples were cooled until they reached room temperature inside the oven. Then, the samples were subjected to a final polishing process [6].

Subsequently, double waveguides were created, consisting of a pair of parallel lines each of which is produced by superimposing four laser-irradiated tracks. These tracks were manufactured using a fs laser system (Ti:sapphire, model PRO 400, Femtolasers GmbH) and a focusing lens with a focal length of 20 mm, N.A = 0.23, with the focal point positioned 0.75 mm below the surface. The laser beam was perpendicular to the polished surface of the sample, with the linear polarization inclined at 45° to the direction of movement, at a speed of 0.5 mm/s and pulse energy of 30 μJ. In this work Ag NPs are produced during the annealing; however, we cannot discard their concentration growth during fs laser irradiation, as already reported in the literature, for tungsten lead–pyrophosphate glass [6, 14]. The two straight waveguides included two parallel straight lines each, separated by distances of 10 and 25 μm, curved waveguides with a radius of curvature of 20 mm and distances of 10 and 25 μm; a Y-shaped waveguide was also produced, with an opening angle of 5º and distance of 620 μm between the arms, maintaining a distance of 10 μm between the guide walls. Curved guides with radius of 5 and 10 mm were produced but demonstrated no guiding. Figure 1, from left to right, displays two curved guides, followed by two straight guides, and the Y-shaped guide.

The structures that form the walls of the double waveguides are formed by regions with a refractive index lower than that of the original glass, and have approximate dimensions of 178 mm x 3 mm [6]. Due to these dimensions and the low contrast with the surrounding medium, these regions are very difficult to observe, and can only be seen with polarized light microscopy, and under special conditions. Therefore, any characterization of the morphology of the walls, such as their roughness, becomes an extremely difficult task and was not done in this work. The laser beam used has a Gaussian distribution, and the pulse overlap rate was quite high, which could indicate a great homogeneity in the morphology of the walls.

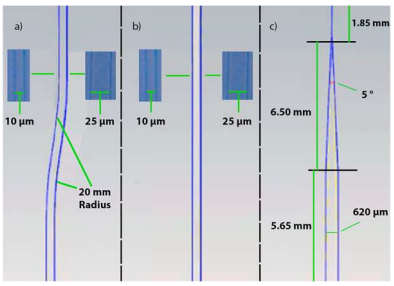

Fig. 1. Illustration of the waveguides configurations irradiated with fs laser in GeO_2PbO glass a) curved b) straight c) Y-shaped.

Using the setup shown in Fig. 2 (a), the propagation losses for all waveguide configurations were measured at 632 nm, using the straight waveguide with 10 μm separation as reference [15]; the output power distribution of the straight waveguide with 25 μm width, the two curved waveguides (with 10 and 25 μm separation between the walls) and also the two arms of the Y waveguide was obtained. Then with equation 1, it was possible to measure the relative propagation losses [15]:

$$\eta = -10 \log_{10}\left(\frac{\sum_i P_i}{P_0}\right) \quad (1)$$

In the equation above P_i is the sum of the output powers of the guide that will be compared, and P_0 represents the output power of the 10 μm waveguide used as a reference. This procedure is suitable as it avoids the use of the cutback method [15-17] but not adequate for samples that cannot be cut, as is the case of those with curved and Y shaped configurations. Finally, η represents the value of the relative losses in dB.

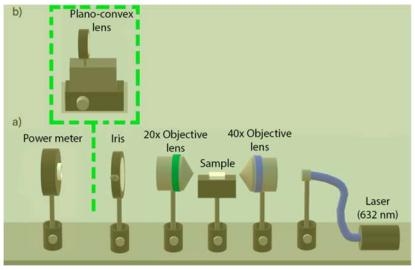

Fig. 2. Experimental setup used to measure a) propagation loss; b) M^2.

To determine the quality of the waveguide output beam, the M^2 was measured for all waveguide configurations, using standard procedures [18] and the setup illustrated in Fig. 2 (b) and replacing the power meter by a CCD camera. Using equation 2 it was possible to determine M^2 by measuring the beam diameter along the near and far fields, obtained for 632 nm [17]. Then the experimental values were adjusted by equation 2 where d = 2w is the diameter of the waveguide output beam (2w) measured at different focal distances (z). The diameter of the beam at the focus (z_0) is given by d=2 w_0.

$$d = d_0 \sqrt{1 + \left(\frac{(M^2 \lambda (z - z_0))}{(\pi {d_0}^2)}\right)^2} \quad (2)$$

Equation 3 is used to calculate M^2 at 1064 nm using the values obtained with the setup of Fig. 2 (b) since $\lambda \ll w$

$$M^2 = \frac{\pi \cdot \theta_{ideal} \cdot w_{0ideal}}{\lambda} \quad (3)$$

In the above equation, θ_{ideal} is the beam divergence semi-angle measured in the far field and $w_{0_{ideal}}$ is the waist radius at the beam focus. Finally, polarization was measured using the experimental arrangement presented in Figure 3. The acquired data made it feasible to calculate a percentage relationship between the power output values of each polarization axis. These results were of importance for the assessment of polarization during the guidance process and its corresponding orientation.

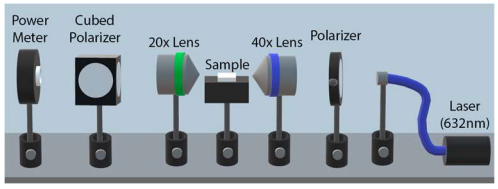

Fig. 3. Experimental setup used for measurements of polarization of dual waveguides.

Optical microscopy was performed to obtain top images of all the waveguides.

III. RESULTS

Table 1 summarizes the values obtained for relative propagation loss (equation 1 and setup of fig. 2a) of each configuration, compared to the straight waveguide of 10 µm, which served as the reference.

TABLE 1 - PROPAGATION LOSSES CONCERNING A STRAIGHT WAVEGUIDE WITH A DISTANCE BETWEEN THE WAVEGUIDE WALLS OF 10 µm.

Waveguide	Propagation losses (dB/cm)
Straight 25 µm	0.74
S curved 10 µm	1.33
S curved 25 µm	2.19
Y waveguide	0.55

By using the arrangement of Fig. 2 (b) it was possible to measure the beam waist (d=2w) as a function of the z position. The results of the M^2 factor at 632 nm obtained by equation 2, for the horizontal and vertical axes, respectively, are presented in Figure 4 (for straight waveguide configuration with 10 µm distance between the walls).

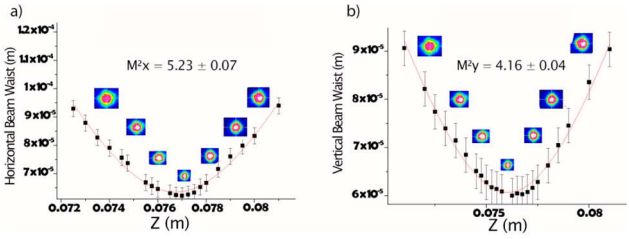

Fig. 4. GP sample results for the straight waveguide with a distance between the guide walls of 10µm a) M²x b) M²y.

The results for all waveguide configurations can be seen in Table 2.

TABLE 2- M^2_X AND M^2_Y VALUES AT 632 nm FOR ALL WAVEGUIDES.

Waveguide	M²x (632 nm)	M²y (632 nm)
S curved 10 µm	15.2	10.64
S curved 25 µm	23.5	28.8
Straight 10 µm	5.23	4.16
Straight 25 µm	6.30	5.31
Y first arm	5.03	6.99
Y second arm	5.84	5.46

Using equation 3 it was possible to obtain the results of the M^2 at 1064 nm, which are presented in Table 3.

TABLE 3 - M^2_X AND M^2_Y VALUES AT 1064 nm FOR ALL WAVEGUIDES.

Waveguide	M²x (1064 nm)	M²y (1064 nm)
S curved 10 µm	9.02	6.32
S curved 25 µm	13.95	17.09
Straight 10 µm	3.11	2.47
Straight 25 µm	3.74	3.15
Y first arm	2.99	4.15
Y second arm	3.46	3.24

Using the setup of Fig 2b) it was determined that the output power ratio between the left and right arms of the Y waveguide was 53.9/46.1, indicating potential photonic applications, such as beam splitters. The polarization results can be seen in Tables 4 and 5, with the input vertical and horizontal polarizations respectively. The polarization measurement was performed for the S curved and straight configurations (with the set up presented in fig. 3) with the smaller distance between the guide walls (10 µm) that presented the smaller losses. Only the S-curved (10 µm) showed horizontal polarization (12%), as presented in Table 4. Regarding the results presented in Table 5, vertical polarizations were observed for the straight waveguide (13%) and for both Y arms (right and left) with polarizations of 10%. The polarization measurement was performed for the S curved and straight configurations (with the setup presented in Fig. 3) with distance between the guide walls of 10 µm that presented smaller losses with respect to those with 25 µm.

TABLE 4 - OUTPUT POLARIZATION PERCENTAGE WHEN INPUT LASER POLARIZATION IS VERTICAL.

Waveguide	Vertical polarization (%)	Horizontal polarization (%)
S curved 10 µm	87.9 ± 0.7	12.1 ± 0.7
Straight 10 µm	98 ± 2	2.3 ± 2.2
Y first arm	98 ± 3	2.3 ± 2.8
Y second arm	97 ± 2	3.1 ± 2.1

TABLE 5 - OUTPUT POLARIZATION PERCENTAGE WHEN INPUT LASER POLARIZATION IS HORIZONTAL.

Waveguide	Vertical polarization (%)	Horizontal polarization (%)
S curved 10 µm	6.7 ± 5.9	93 ± 6
Straight 10 µm	13 ± 2	87 ± 2
Y first arm	10 ± 1	90 ± 1
Y second arm	10 ± 4	90 ± 4

The results obtained by optical microscopy (top images) can be seen in Fig. 5a and Fig 5b for the straight waveguide with 10 and 25 µm distance between the guide walls. The results for the two curved waveguides, separated by 10 and 25 µm are presented in Fig. 6a and 6b, respectively. The corresponding output modes are also shown.

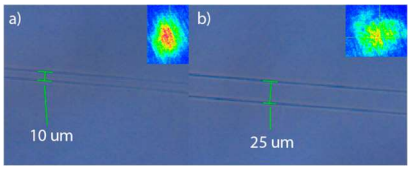

Fig. 5. Top images and the corresponding output modes of the straight waveguide with a distance between the guide walls of a) 10 µm b) 25 µm.

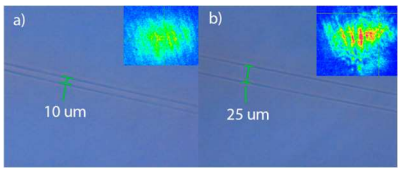

Fig. 6. Top images and the corresponding output modes of the curved waveguides with a distance between the guide walls of a) 10 µm b) 25 µm.

Fig. 7 presents the microscopy results of the Y waveguide and the simultaneous view of the output modes of the two arms.

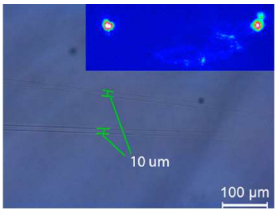

Fig. 7. Top images of the two arms of the Y waveguide and the corresponding output modes.

IV. Conclusion

In short, with the analysis of the data, it was possible to observe a better result in the straight waveguide configuration with respect to propagation losses and beam quality. Other than that, the distance between the guide walls resulted in higher output powers when the distance was smaller (10 μm) for both straight and curved waveguides. Also, for both, straight and S curved waveguides, better M^2 results were found for a distance between the guide walls of 10 μm, when compared with 25 μm. Moreover, for curved guides it was also possible to observe better guidance when they had a larger radius of curvature, since in the initial tests with 5 mm and 10 mm radius, there was no light guidance. The highest propagation loss was obtained for the S curved guide with a 25 μm distance between the guide walls. We highlight the low propagation losses in both arms, for the Y configuration. Finally, the configuration of a Y waveguide showed promising results for applications in photonics, such as beam splitters due to the output power ratio between the left and right arms being close to 50%. In this configuration, an opening angle of 5° and 620 μm was used between the two arms. The present results show for the first time the possibility of producing passive waveguides with curved and Y configurations, using GeO_2-PbO glass with Ag NPs, and the configuration of double waveguides each formed by 4 superpositions. Most of the results reported in the literature for curved and Y waveguide configurations are mainly produced in crystalline hosts. The present investigation covers a lack in the literature related to curved and Y-shaped waveguides irradiated by fs laser in glasses and can be extended to different glassy hosts with Ag NPs.

Acknowledgments

This study was financed in part by the Coordenação de Aperfeiçoamento de Pessoal de Nível Superior – Brasil (CAPES) – Finance Code 001, and CAPES-PROEX 88887.670647/2022-00. We acknowledge Conselho Nacional de Desenvolvimento Científico e Tecnológico—Grants 465.763/2014 (Instituto Nacional de Ciência e Tecnologia de Fotônica), 305745/2023-9, 308526/2021-0 and also Fundação de Amparo à Pesquisa do Estado de São Paulo—Grants: 2019/06334-4, 2017/10765-5, Sisfóton-Grant 440.228/2021-2.

References

[1] M. Wachtler, et al. “Phonon Sidebands and Vibrational Properties of Eu^{3+} Doped Lead Germanate Glasses.” Journal of Non-Crystalline Solids, vol. 217, no. 1, pp. 111–114, 1997.

[2] M. Wachtler, et al. “Optical Properties of Rare-Earth Ions in Lead Germanate Glasses.” Journal of the American Ceramic Society, vol. 81, no. 8, pp. 2045–2052, 2005.

[3] C.B. De Araújo and L. R. P. Kassab. “Enhanced Photoluminescence and Planar Waveguide of Rare-Earth Doped Germanium Oxide Glasses with Metallic Nanoparticles.” Glass Nanocomposites, pp. 131–144, 2016.

[4] L. De Boni, et al. “Femtosecond Third-Order Nonlinear Spectra of Lead-Germanium Oxide Glasses Containing Silver Nanoparticles.” Optics Express, vol. 20, no. 6, pp. 6844–6844, 2012.

[5] D.S. Da Silva, et al. “Production and Characterization of Femtosecond Laser-Written Double Line Waveguides in Heavy Metal Oxide Glasses.” Optical Materials, vol. 75, pp. 267–273, 2018.

[6] C.D.S Bordon, et al. “Effect of Silver Nanoparticles on the Optical Properties of Double Line Waveguides Written by Fs Laser in Nd^{3+} -Doped GeO_2-PbO Glasses.” Nanomaterials, vol. 13, no. 4, pp. 743–743, 2023.

[7] C.D.S. Bordon, et al. “A New Double-Line Waveguide Architecture for Photonic Applications Using Fs Laser Writing in Nd^{3+} Doped GeO_2-PbO Glasses.” Optical Materials, vol. 129, pp. 112495–95, 2022.

[8] L. Li, et al. “Femtosecond-Laser-Written S-Curved Waveguide in Nd:YAP Crystal: Fabrication and Multi-Gigahertz Lasing.” Journal of Lightwave Technology, vol. 38, no. 24, pp. 6845–6852, 2020.

[9] H.-D. Nguyen, et al. “Heuristic Modelling of Laser Written Mid-Infrared $LiNbO_3$ Stressed-Cladding Waveguides”. Vol. 24, no. 7, pp. 7777–7791, 2016.

[10] A. Abou Khalil, et al. “Direct Laser Writing of a New Type of Waveguides in Silver Containing Glasses.” Scientific Reports, vol. 7, no. 1, 2017.

[11] V. A. Amorim, et al. “Optimization of Broadband Y-Junction Splitters in Fused Silica by Femtosecond Laser Writing.” IEEE Photonics Technology Letters, vol. 29, no. 7, pp. 619–622, 2017.

[12] A. Yalcin, et al. “Optical Sensing of Biomolecules Using Microring Resonators.” IEEE Journal of Selected Topics in Quantum Electronics, vol. 12, no. 1, pp. 148–155, 2006.

[13] R. Dangel, and W. Lukosz. “Electro-Nanomechanically Actuated Integrated-Optical Interferometric Intensity Modulators and 2×2 Space Switches”. Vol. 156, no. 1-3, pp. 63–76, 1998.

[14] J.M.P Almeida, et al. “Metallic Nanoparticles Grown in the Core of Femtosecond Laser Micromachined Waveguides.” Journal of Applied Physics, vol. 115, no. 19, pp. 193507, 2014.

[15] J.R.V. De Aldana, et al. “Femtosecond Laser Direct Inscription of 3D Photonic Devices in Er/Yb-Doped Oxyfluoride Nano-Glass Ceramics.” Optical Materials Express, vol. 10, no. 10, pp. 2695, 2020.

[16] D.L. Yang, et al. “Radiative Transitions and Optical Gains in Er^{3+}/Yb^{3+} Codoped Acid-Resistant Ion Exchanged Germanate Glass Channel Waveguides.” Journal of the Optical Society of America B-Optical Physics, vol. 26, no. 2, pp. 357–357, 2009.

[17] E.C. Sousa. “Otimização Da Eficiência Do Modo TEM00 Em Lasers de Nd:YLF de Alta Potência Bombeados Lateralmente”. IPEN, São Paulo, vol. 89, pp. 22 – 24, 2008.

[18] D. Feise, et al. “High-Brightness 635nm Tapered Diode Lasers with Optimized Index Guiding.” Proc. SPIE 7583, High-Power Diode Laser Technology and Applications VIII, vol. 75830. SPIE, 2010